Identification of key residues in water channel formation in the *Bacillus subtilis* germinant receptor protein GerAB

Longjiao Chen[1,2], Houdijn Beekhuis[2], Christina van den Bosch[1], Gianni Vinay[1], Jocelyne Vreede[2#], Peter Setlow[3#], Stanley Brul[1#]

[1] Swammerdam Institute of Life Sciences, University of Amsterdam, Science Park 904, 1098 XH, Amsterdam

[2] Van 't Hoff Institute for Molecular Sciences, University of Amsterdam, Science Park 904, 1098 XH, Amsterdam

[3] Department of Molecular Biology and Biophysics, UConn Health, 263 Farmington Avenue, Farmington, CT 06030-3305

[#] These authors contributed equally

Abstract

Some species in the *Bacillales* and *Clostridiales* bacterial orders form spores in unfavorable environments. These spores are metabolically dormant, and resistant to harsh conditions. However, upon triggering by a variety of small molecule nutrients, termed germinants, spores may germinate, increasing their core water content from 25%-45% in spores to ~80% in growing cells, thus restoring rapid metabolism and leading to outgrowth and then vegetative growth. Recent structural modeling and mutagenesis studies showed that a subunit of the prototypical *Bacillus subtilis* spore germinant receptor (GR) GerA, the integral inner membrane (IM) protein GerAB, is involved in spore germination initiated by L-alanine. Notably, a previous molecular simulation study showed the formation of a water channel in GerAB. In the current study we employed Steered Molecular Dynamics (SMD) simulations to force a single water molecule through GerAB. Examining the simulations revealed three key amino acid residues, Y97, L199 and F342, that interfere with water passage. These three residues were altered to alanine, followed by assays of germination. In the Y97A, L199A, F342A single mutants and the Y97A, L199A and F342A triple mutant (triA), all four types of mutant spores barely responded to L-alanine, while wild type spores germinated almost 100% under the same conditions. Y97A spores expressed the GerAA protein as determined by western blot analysis, corroborating the presence of the GerA GR. However, for the other three mutants, GerAA's presence in the spore could not be confirmed. In conclusion, Y97 plays a key role in GerAB mediated germination and suggests that GerAB indeed facilitates water passage and further indicating that water passage through GerAB is a crucial event in *B. subtilis* spore germination.

Introduction

Several species within the *Bacillales* and *Clostridiales* bacterial orders can form dormant spores in harsh environments. These spores are metabolically inert, extremely resistant to a variety of harsh treatments, and dormancy can last for decades. However, cells derived from some of these spores can cause food spoilage, infectious diseases, intoxications and foodborne illnesses[1]. This holds true for spores of *Bacillus anthracis*, *Clostridiodes difficile* and *Bacillus cereus,* respectively. Consequently, the biology of spore-forming bacteria has been intensively studied for decades. A major feature of dormant spores is their very low central core

water content, 25%-45% of wet weight (wt.), in spores of the model organism *Bacillus subtilis* compared to ~80% of wet wt. in growing cells. However, how water is taken up into the dormant spore core is not clear, as *B. subtilis* lacks known water pores such as aquaporins[2,3].

The loss of spore dormancy and resumption of its metabolism and cell-like structure requires spore germination, in which spore core water content increases at least 45% wet wt. small molecule nutrients, including specific monosaccharides, monovalent cations, and amino acids, can trigger spore germination, although germinant catabolism is not involved[4]. Germinant receptors (GRs) play a crucial role in kick-starting germination. In the model organism *B. subtilis*, the major GR, GerA, is composed of three subunits, called A, B, and C. The B subunit GerAB is a transmembrane protein that mediates L-alanine triggered germination[5–7]. The three subunits work closely together and all three are essential for functional GerA formation[1,4]. Blinker *et al.* identified a putative water channel in GerAB using molecular dynamics (MD) simulations[8]. A recent study by Gao *et al.* showed that using a combination of AlphaFold[9] structure prediction and mutagenesis results in GerA forming an oligomeric membrane channel which releases monovalent cations upon sensing L-alanine[10]. However, to date, the function and mechanism of spore water intake during germination facilitated by GerAB has not been fully clarified.

In order to investigate the molecular mechanism of GerAB mediated water uptake, MD simulation studies coupled with experimental mutagenesis and spore germination assays have been carried out. First, water molecules were pulled through GerAB from the outside of the inner membrane (IM) to its inside in Steered Molecular Dynamics (SMD) simulations. In these simulations, the termini of GerAB are assumed to be located on the inside of the spore[10] (Figure 1). During these SMD simulations, the work required for pulling a water molecule through GerAB was measured. Visual inspection of the SMD trajectories showed that three amino acid residues Y97, L199 and F342 interfere with the passage of water through GerAB. The sidechains of these residues are close to one another and act as obstacles to water passage. To verify the role of these residues, spores of mutants Y97A, L199A, F342A and triA (Y97A, L199A and F342A triple mutant) were prepared, and the germination efficiencies of the wild type and mutant spores were measured by phase contrast microscopy. With L-alanine as germinant, wild type spores germinated almost 100% while all of the four mutant spores germinated poorly (no more than 20%) under the same conditions. Western blotting verified that both wild type and Y97A spores contained GerAA, while the other three mutants did not, indicating that only the wild type and Y97A mutant spores could assemble the complete GerA GR. Together, these observations provide evidence that GerAB acts as a water channel in which Y97 plays a key role in water passage through this GR subunit.

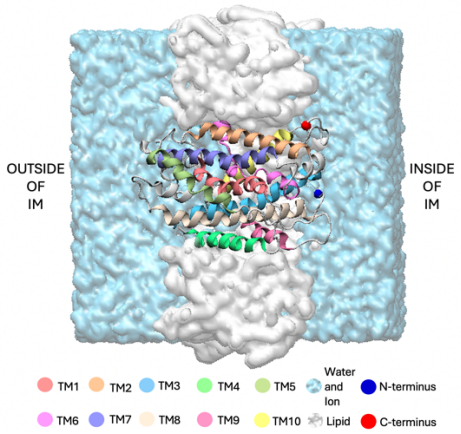

Figure 1. The simulations system used in this study. The GerAB protein is inserted in a lipid double layer membrane (shown as a white surface), with its N- and C-termini located on the inside of the spore IM. The protein is shown as ribbon, with the 10 TMs (Transmembrane helices) separately colored. Water and 20 mM of KCl are shown as blue surface.

Materials and Methods

1 Simulations and analysis

One 100 ns molecular dynamics (MD) simulation of a protein structure model based on *Methanocaldococcus jannaschii* ApcT (PDB: 3GI8)[11] generated by the structure prediction tool raptorX[12] was conducted using the same starting structure and settings as those described by Blinker *et al*[8]. The simulation was performed with GROMACS 2020.4[13], using the CHARMM36[14] forcefield. In a cubic periodic box with dimensions of 10 by 10 by 11 nm, the system was solvated by TIP3P water molecules[15]. The simulation was maintained at a temperature of 298 K using the Bussi velocity rescaling thermostat[16] and at constant pressure of 1.0 bar with the Parrinello-Rahman barostat[17,18]. Long-range electrostatic interactions were treated using the Particle Mesh Edward[19] method with a maximum grid spacing at 1.6 Å. For short-range electrostatic and Van-der-Waals interactions the cutoff radius was set to 12 Å. The production run lasted 100 ns with a timestep of 2 fs, with coordinates saved every 2 ps. The term "(free) MD simulation" refers to the MD simulation production run conducted for this research.

Steered Molecular Dynamics (SMD) simulations were performed to pull a water molecule through the protein, using 10 starting structures extracted every 10 ns from the MD simulation. With the protein located in the center of the simulation box (protein center of mass at 4.76 nm ~ 4.85 nm at x and y coordinate, and the membrane boundaries at 3.0 nm < z < 7.0 nm, the entrance of the water channel was defined as 3.5 nm < x < 6.5 nm, 3.5 nm < y < 6.5 nm and 4.6 nm < 6.1 nm. In each starting frame, a water molecule was selected with the coordinates of its oxygen atom within the entrance range. The steered MD simulations were conducted using PLUMED 2.7.0[20–22] embedded with GROMACS 2020.4, where the steering collective variable (CV) was the position in the z-direction of the oxygen atom of the pulled water molecule. In all SMD simulations, the selected water molecule was pulled 4 nm over 100 ns along the z-

coordinate towards the inside of the inner membrane (IM), following the direction of water intake during germination. Over the 100 ns simulation, a moving harmonic potential kept the water oxygen constrained to z with a force constant κ = 10000 kJ mol^{-1} nm^{-2}. The harmonic restraint moved at a constant velocity of 0.04 nm/ns. In addition, the water oxygen atom was constrained in the x and y direction with a harmonic potential with a force constant κ = 10 kJ mol^{-1} nm^{-2}, to keep the water molecule inside the protein. The SMD simulations were performed with the same settings as the MD simulation. The work performed to constrain the water molecule along the z coordinate in the SMD simulations was computed as the cumulative force applied to the water molecule over the simulation time. In total, 10 SMD runs were performed. Visual inspection of the simulation trajectories was conducted using Visual Molecular Dynamics (VMD) 1.9.4a53[23].

3 Mutagenesis

All strains were derived from *Bacillus subtilis* PY79. The *gerA* operon was cloned by PCR, inserted in plasmid vector pUC19 with the Gibson Assembly Master Mix kit (New England BioLabs, NEB # E2611S). Mutagenesis was carried out with the QuikChange Lightning Site-Directed Mutagenesis Kit (Agilent Technologies, Cat # 210518-5). Mutant *gerAB* sequences were integrated into the original *gerAB* locus by a double crossover along with an erythromycin (erm) resistance cassette. The correct sequence of various mutant *gerAB* loci were confirmed by Sanger sequencing. Mutant strains generated in this study are listed in Table 1. In addition to the mutant described above, a G25A and a G200A mutant[7,24] were also constructed as control strains as the mutated residues are not interfering with water passage according to the current study.

Table 1. Strains constructed in this study.

GerAB variant	Strain
Wild Type (wt)	*Bacillus subtilis* PY79
Y97A Erm	*Bacillus subtilis* PY79
L199A Erm	*Bacillus subtilis* PY79
F342A Erm	*Bacillus subtilis* PY79
triA (Y97A L199A F342A triple mutant) Erm	*Bacillus subtilis* PY79
G25A Erm	*Bacillus subtilis* PY79
G200A Erm	*Bacillus subtilis* PY79

4 Sporulation and spore purification

All strains were grown to give single colonies on an LB-agar plate. A single colony was transferred to 5 ml LB medium (pH 7.5) and grown at 37°C; after the OD_{600} reached 0.3-0.4, serial 10-fold dilutions were incubated overnight in 8 mM MOPS minimal medium (K_2HPO_4 1.32 mM, $MgCl_2$ 0.4 mM, K_2SO_4 0.276 mM, $FeSO_4$ 0.01 mM, $CaCl_2$ 0.14 mM, MOPS 8 mM, Tricine 4 mM, pH 7,5)[24]. 1 ml of the dilution with OD_{600} at ~ 0.3-0.4 was further diluted 20-fold in prewarmed MOPS minimal medium (pH 7.5). The culture was kept at 37°C while shaking at 200 rpm until the OD_{600} reached 0.3-0.4. To obtain the spore crop, 1% of the obtained (v/v) pre-culture was inoculated into the final sporulation MOPS (8 mM) minimal medium and incubated for three days at 37°C while shaking at 200 rpm. The culture was then pelleted by centrifugation at 5000 rpm for 15 min at 4°C. The pellet was resuspended in sterile milliQ (MQ) water and centrifuged at 5000 rpm for 15 min at 4°C. This washing step was repeated 2-3 times. To remove vegetative cells the spores were suspended in 20% Histodenz and loaded onto 50%

Histodenz. The loaded samples were centrifuged at 15000 rpm for 60 min (4°C) and the supernatant was discarded. This step was then repeated to remove any germinated spores. Again, the supernatant was discarded, and the pellet was resuspended in MQ water and washed 2-3 times. Finally, the retrieved spores were diluted to an OD_{600} of approximately 50 in 1 mL MQ water and samples were stored at -80°C.

5 Phase contrast microscopy and analysis

Purified phase-bright spores at OD_{600} of 5 in MQ water were heat-activated at 70°C for 30 min followed by 20 min incubation on ice. Before the addition of the germinants, the germinant solutions were kept on ice. A final concentration of 1 mM L-alanine or 50% of AGFK solution (13.22 mg/ml L-asparagine, 55.48 mg/ml D-glucose monohydrate, 50.44 mg/ml D-fructose, 37.28 mg/ml potassium chloride) [7,25] was added prior to slide preparation and imaging according to Wen et al.[24] In essence, to prepare a slide for wide field imaging, a slide and cover glass were removed from storage, cleaned with 70% EtOH and air dried in a vertical position minimizing dust collection. Meanwhile, two coverslips were prewarmed for several seconds on a 70°C heating block, 65 µl 2% agarose was deposited on top of one slide, while the other slide was placed perpendicular to it, spreading the agarose between the slides. The agarose patch was dried for approximately 10 min, after which the slides were slid off each other. The agarose patch was cut into a 1x1cm section to which 0.4 µl of normalized spore suspension with germinant was added. The patch was transferred onto the coverslip by placing the coverslip onto the patch and sliding it off. A G-frame was stuck onto the air-dried slide, onto which the coverslip was placed, closing all corners of the frame, and completing the slide for microscopy. For wide field time-lapse experiments, we used a Nikon Eclipse Ti equipped with a Nikon Ti Ph3 phase contrast condenser. Connected to it were a Nikon Plan Apo Plan Apo λ Oil Ph3 DM lens (100X, NA=1.49, T = 23°C), a Lumencor Spectra Multilaser (470 nm, 555 nm) using Lambda 10-B filter blocks, a NIDAQ Lumencor shutter, a Ti XY-and Z drive, and a Hamamatsu C11440-22C camera. All hardware was connected to a computer running NIS-Elements AR 4.50.00 (Build 1117) Patch 03. Before every use the condenser was adjusted to the optimal setting bringing the pixel size to 0.07 µm per pixel. A 100-minute time lapse video was recorded for every slide, with the slide chamber kept at 37°C, and germination was analyzed with SporeTrackerX[26]. The percentages of germinated spores within the time of microscopy were measured as germination efficiency.

6 SDS-PAGE and immunoblotting

To prepare samples for western blotting, the spores were first decoated and then lysed as follows. 50 ODs of spores were pelleted by centrifugation. The pelleted spores were resuspended in 1 mL TUDSE buffer (8 M Urea, 50 mM Tris-HCl, pH 8.0, 1% SDS, 50 mM DTT, 10 mM EDTA) and incubated for 45 minutes at 37˚C, centrifuged (3 min, max rpm, room temperature) and resuspended in 1 mL TUDS (8 M Urea, 50 mM Tris-HCl, pH 8.0, 1% SDS) buffer. The suspension was then incubated for another 45 minutes at 37˚C, centrifuged (3 min, max rpm, room temperature) and then washed six times by centrifugation (3 min, max rpm, room temperature) and then all suspended in 1 mL TEN buffer (10 mM Tris-HCl pH 8, 10 mM EDTA, 150 mM NaCl). The final decoated spores were resuspended in 1mL water if samples were not immediately given further treatment right afterwards. 50 OD of the decoated spore preparation was treated with 1mg lysozyme in 0.5mL TEP buffer (50 mM Tris-HCl pH 7.4, 5 mM EDTA) containing 1mM phenylmethylsulfonyl fluoride (PMSF), 1µg RNase, 1

μg Dnase I, and 20 μg of MgCl2 at 37°C for 6 to 8 min, and then put on ice for 20 min. Glass disruptor beads (0.10 to 0.18 mm, 100 mg) were added to each sample and spores were disrupted with three bursts of sonication (micro probe, medium power, 10 sec, placed on ice for 30 sec. between bursts). Following the final sonication pulse, samples were allowed to settle for 15 sec and 100 μl was withdrawn and added to 100 μl 2x Laemmli sample buffer (BIO-RAD cat. #1610737) containing 5% (v/v) 2-mercaptoethanol and 1 mM $MgCl_2$ and incubated at 90-95°C for 3 min. This was saved as the total lysate and ready to run on SDS-PAGE. 20 μg of total protein was loaded onto each lane of SDS-PAGE on a 10% acrylamide gel (BIO-RAD cat. #4561034) and run 45 min at 60 V followed by 45 min at 110 V. After SDS-PAGE, proteins on the gel were transferred to a 0.22 μm PVFD membrane. The film was blocked by 2.5% low fat milk in TBST buffer (20 mM Tris, 150 mM NaCl, 0.1% Tween 20) and incubated with 1:3000 anti-GerAA antibody overnight[27]. After washing three times with TBST, the film was incubated with 1:2500 goat anti rabbit HRP antibody (BIO-RAD cat. #1706515) for an hour before visualization.

Results

1. Key residue identification

In the SMD simulations, water molecules were pulled through GerAB from the outside of the spore to the inside of the spore, as indicated in Figure 2A. For each individual SMD run, the cumulative work as a function of the z coordinate was calculated. For all runs, the exerted work increases after z = 5 – 5.5 nm until a z-coordinate between 6.5 and 7.5 nm. This means that the water molecule does not go spontaneously through the protein at the pulling speed. At z > 6.5 nm, the cumulated work stays approximately constant, which means that no additional work is required to pull the water molecule through bulk water after it has exited the protein (Figure2B). This observation shows that the SMD does not suffer from artefacts caused by pulling the water too fast, as pulling the water molecule through bulk water happens at a velocity typical for water diffusion at 298 K[28]. This indicates that the pulling speed is sufficiently slow.

The pulling work profiles all have a similar shape but differ in when the plateau is reached. To quantify this variation, the difference of the cumulative work is defined as $\Delta w = w_{end} - w_{start}$. Δw ranged from Δw_{min}= 41.69 kJ/mol to Δw_{max}= 275.43 kJ/mol (Figure 2B). According to the Boltzmann distribution, the process requiring the least amount of work is the most likely to occur during the process of water passage[29]. Consequently, we visually inspected the run with the smallest Δw, labeled Δw_{min}. In this simulation, a group of three amino acids with bulky side chains (termed triad, consisting of Tyr97, Leu199, and Phe342, Figure 2C) blocked the movement of the water molecule along the z-axis. To continue moving through GerAB, the water molecule bypassed the triad between TM3 and TM6 where Tyr97 and Leu199 are located, respectively (Figure 2D). On the contrary, in all the other SMD simulation trajectories, the water was pulled through the three bulky side chains of the triad, with run Δw_{max} as an example (Figure 2E).

In summary, the bulky side chain triad interfered with water passage in all the SMD simulations trajectories. We also observed that the pulling work varies between the runs, and that the water paths are different for the lowest work simulation Δw_{min} and the other simulations. These results indicate that the triad may play a role in water passage. To verify the function of the triad *in vivo*, we hypothesized that by mutating the triad residues to alanine, we remove the bulky side chains, and therefore construct mutant spores with an aberrant water passage profile, such as for example a leaky channel which would lead to a spontaneous germinating phenotype.

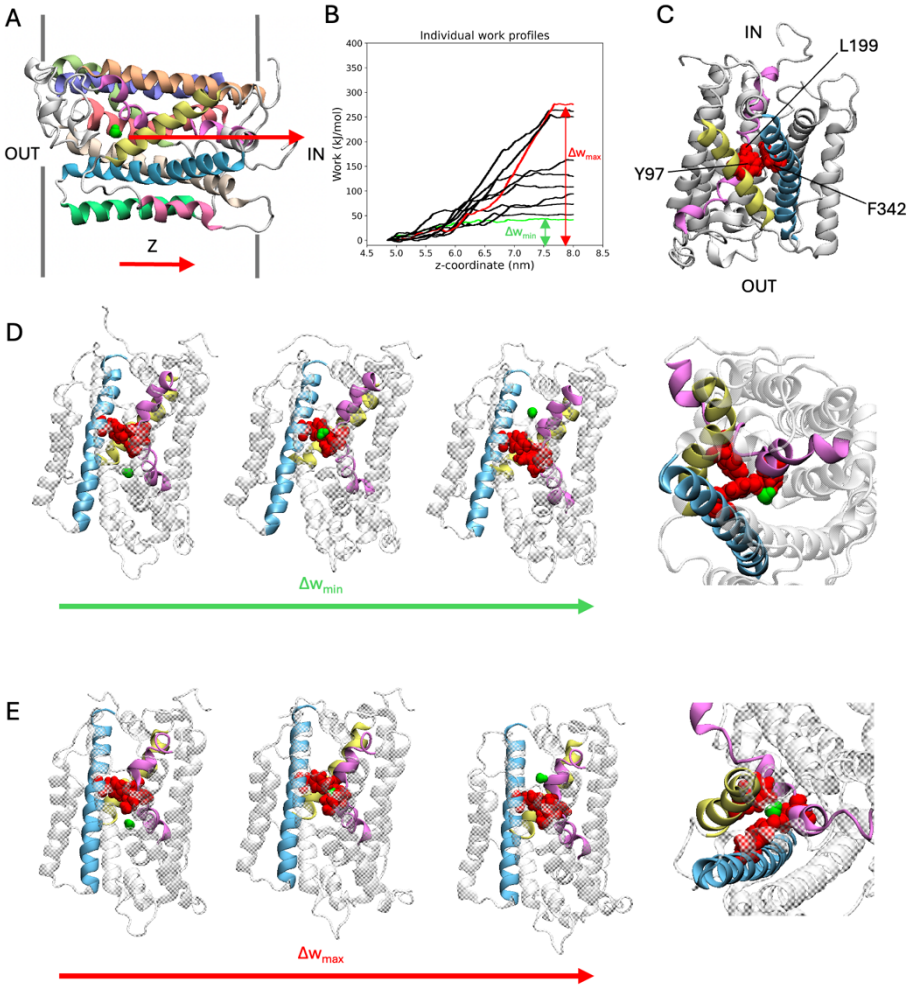

Figure 2. (A) Example starting frame for the SMD simulations. The water molecule which is pulled is shown in green spacefilling representation. The arrow indicates the pulling direction, from the outside of the spore IM to the inside. Dark grey lines flanking the protein indicate the membrane. (B) Work profiles of the SMD simulations along the z-axis. The work profiles Δw_{max} and Δw_{min} are shown in red and green, respectively. (C) A triad of Tyr97, Leu199, and Phe342 (all in red spacefilling representation) are located on TM3, TM6, and TM10, respectively. Only TMs with triad are colored, according to the coloring scheme in Figure 1. Protein regions not part of the triad is shown in white. (D), (E), Water molecule passing the triad in the SMD simulation with Δw_{min} and Δw_{max}, respectively. From left to right: snapshots of simulation for water oxygen at z = 4.84 nm, 5.89 nm, 6.65 nm (for Δw_{min}), and z = 5.07 nm, 6.21 nm, 7.84 nm (for Δw_{max}), showing the water before, during, and after passing the triad, followed by a closeup of the triad with the

water molecule during water molecule passing the triad. The closeup is shown from the inside of the spore.

3. GerAB Y97A influences germination efficiency of *B. subtilis* spores

Six mutant strains of *B. subtilis* PY79 were successfully constructed and verified by sequencing. Residues in the triad were replaced by alanine, one at a time, to understand if the "interference" of the bulky side chains could affect the water intake of the spore upon L-alanine or AGFK-induced spore germination. The six mutants include: Y97A, L199A, F342A, triA (Y97A, L199A and F342A triple mutant). In addition, we included G25A and G200A[7] as controls. In G25A interaction with L-alanine in GerAB is known to be perturbed while G200A is known to lead to a lack of detectable GerA GR all together.

The differences in germination efficiency of each strain with L-alanine or the AGFK (mixture of L-asparagine, D-glucose, D-fructose and K^+ ions)[25] shows that each one of the mutated residues have an important role in L-alanine mediated germination because of the inability to sense L-alanine effectively, either because of the malfunctioning of the water channel, or the latter's important role in GerAB and thus the GerA GR integrity. (Figure 3A) Compared to the wild type, where approximately all the spores germinated, all the mutant spores were only able to germinate with low efficiency with L-alanine (no more than 20%). We next performed western blot analysis of the mutant spores with a purified GerAA antibody, in which only wild type spores and Y97A mutant spores exhibited strong GerAA signals, albeit the level in the mutant is slightly lower than that in wild type spores (Figure 4). This means that the low response of L-alanine of the other mutant spores was due to the absence of GerA GR[30], while in Y97A mutant spores, with GerA GR present, this mutant could alter the germination efficiency of the spores without disrupting the putative L-alanine binding pocket of GerAB[7], thereby providing strong evidence that GerAB acts as a water channel. Besides, only spores of Y97A mutant germinated with AGFK in a comparable level to that of wild type spores, while an approximately 10%-20% drop of germination efficiency with AGFK was observed with other mutant spores (Figure 3B). As AGFK is sensed by the GerB and GerK, GRs with no involvement of GerAB, corroborating with GerA GR only present in Y97A mutant, this indicates that the absence of GerA GR could affect the ability of GerB and GerK GR sensing AGFK. This is not a surprising result since different GRs in *B. subtilis* spores work synergistically[31,32]. However, the germination defect in Y97A mutant spore is contradictory to our initial hypothesis, which indicates instead of creating a large cavity in GerAB and increasing its permeability, this mutation lowered the capability of GerAB to facilitate water passage.

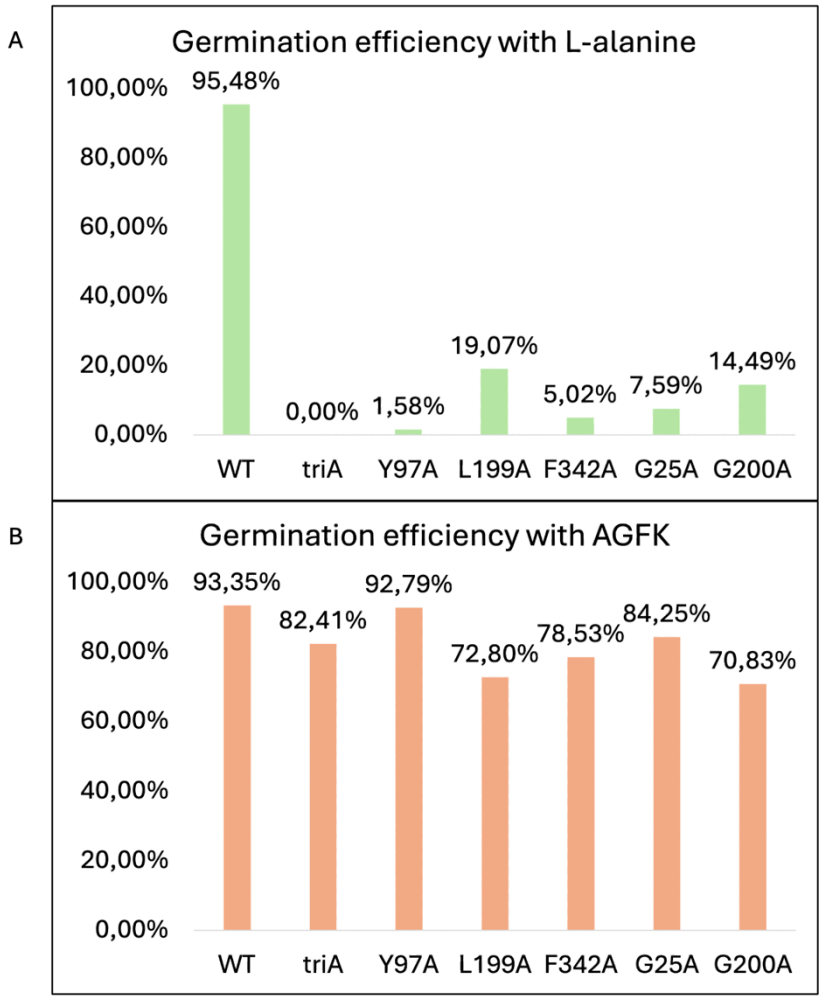

Figure 3. Germination efficiency of spores with different GerAB variants with AGFK (A) or L-alanine (B). Wild type spore reacted almost 100% to both germinant conditions. All mutants respond only poorly to L-alanine. Only Y97A spores responded to AGFK to a comparable level of wild type spores, while other mutant spores exhibit a 10% to 20% drop of germination efficiency to AGFK compared to wild type spores.

Figure 4. Western blot of wild type *B. subtilis* PY79 strain and Y97A strain against GerAA antibody. The blue dot indicates the GerAA band at 50kDa, both samples show a clear band with the GerAA antibody.

Conclusion and Discussion

In this study, the function of GerAB was studied by both SMD and mutagenesis. By pulling a single water molecule through GerAB in a SMD approach, we discovered that the side chains of Y97, L199 and F342, named triad in this study, interfere with water passage. The SMD further revealed two different ways of interaction between water molecule and the triad. In the simulation with the lowest pulling work (Δw_{min}= 41.69 kJ/mol), the water molecule moved through GerAB bypassing the triad between TM3 and TM6. The simulation with the highest pulling work (Δw_{max}= 275.43 kJ/mol) showed the water molecule passing through the three bulky residue sidechains of the triad. Note that these observations are qualitative, to point out different mechanisms of water passing through GerAB. For quantitative results, *i.e.* a free energy profile, several more SMD simulations need to be carried out, as to reduce the variance.

On the other aspect of our work, mutagenesis of GerAB followed by western blot analysis, we verified that Y97 is a key residue in GerAB germination as the GerA GR was still present. However, when sporulating the Y97A strain by a different method, namely on 2 × SG agar plates[33], the alanine germination kinetics of the Y97A mutant spores are similar to those of wild type spores (Prof. Peter Setlow, personal communication). This might be due to the rigidity of spores' IM varying between spores made by different methods with attendant effects on IM proteins, which requires further investigation. Also, to understand the exact role of Y97 in the function of GerAB, mutating Y97 to different residues might give us further insight. Moreover, future simulation work will provide detailed understanding of the mechanism of the interaction between water and GerAB, and how these interactions contribute to the chain of molecular events during spore germination.

References

1. Christie, G., and Setlow, P. (2020). Bacillus spore germination: Knowns, unknowns and what we need to learn. Cell Signal *74*, 109729. https://doi.org/10.1016/j.cellsig.2020.109729.

2. Knudsen, S.M., Cermak, N., Delgado, F.F., Setlow, B., Setlow, P., and Manalis, S.R. (2015). Water and Small-Molecule Permeation of Dormant Bacillus subtilis Spores. J. Bacteriol. *198*, 168–177. https://doi.org/10.1128/jb.00435-15.

3. Sunde, E.P., Setlow, P., Hederstedt, L., and Halle, B. (2009). The physical state of water in bacterial spores. Proc. Natl. Acad. Sci. *106*, 19334–19339. https://doi.org/10.1073/pnas.0908712106.

4. Moir, A., and Cooper, G. (2015). Spore Germination. Microbiol. Spectr. *3*. https://doi.org/10.1128/microbiolspec.tbs-0014-2012.

5. Yi, X., and Setlow, P. (2010). Studies of the commitment step in the germination of spores of bacillus species. J. Bacteriol. *192*, 3424–3433. https://doi.org/10.1128/jb.00326-10.

6. Zuberi, A.R., Moir, A., and Feavers, I.M. (1987). The nucleotide sequence and gene organization of the gerA spore germination operon of Bacillus subtilis 168. Gene *51*, 1–11. https://doi.org/10.1016/0378-1119(87)90468-9.

7. Artzi, L., Alon, A., Brock, K.P., Green, A.G., Tam, A., Ramírez-Guadiana, F.H., Marks, D., Kruse, A., and Rudner, D.Z. (2021). Dormant spores sense amino acids through the B subunits of their germination receptors. Nat Commun *12*, 6842. https://doi.org/10.1038/s41467-021-27235-2.

8. Blinker, S., Vreede, J., Setlow, P., and Brul, S. (2021). Predicting the Structure and Dynamics of Membrane Protein GerAB from Bacillus subtilis. Int J Mol Sci *22*, 3793. https://doi.org/10.3390/ijms22073793.

9. Jumper, J., Evans, R., Pritzel, A., Green, T., Figurnov, M., Ronneberger, O., Tunyasuvunakool, K., Bates, R., Žídek, A., Potapenko, A., et al. (2021). Highly accurate protein structure prediction with AlphaFold. Nature *596*, 583–589. https://doi.org/10.1038/s41586-021-03819-2.

10. Gao, Y., Amon, J.D., Artzi, L., Ramírez-Guadiana, F.H., Brock, K.P., Cofsky, J.C., Marks, D.S., Kruse, A.C., and Rudner, D.Z. (2023). Bacterial spore germination receptors are nutrient-gated ion channels. Science *380*, 387–391. https://doi.org/10.1126/science.adg9829.

11. Shaffer, P.L., Goehring, A., Shankaranarayanan, A., and Gouaux, E. (2009). Structure and Mechanism of a Na+-Independent Amino Acid Transporter. Science *325*, 1010–1014. https://doi.org/10.1126/science.1176088.

12. Källberg, M., Wang, H., Wang, S., Peng, J., Wang, Z., Lu, H., and Xu, J. (2012). Template-based protein structure modeling using the RaptorX web server. Nat. Protoc. *7*, 1511–1522. https://doi.org/10.1038/nprot.2012.085.

13. Abraham, M.J., Murtola, T., Schulz, R., Páll, S., Smith, J.C., Hess, B., and Lindahl, E. (2015). GROMACS: High performance molecular simulations through multi-level parallelism from laptops to supercomputers. SoftwareX *1*, 19–25. https://doi.org/10.1016/j.softx.2015.06.001.

14. Aguayo, D., González-Nilo, F.D., and Chipot, C. (2012). Insight into the Properties of Cardiolipin Containing Bilayers from Molecular Dynamics Simulations, Using a Hybrid All-Atom/United-Atom Force Field. J. Chem. Theory Comput. *8*, 1765–1773. https://doi.org/10.1021/ct200849k.

15. Mark, P., and Nilsson, L. (2001). Structure and Dynamics of the TIP3P, SPC, and SPC/E Water Models at 298 K. J. Phys. Chem. A *105*, 9954–9960. https://doi.org/10.1021/jp003020w.

16. Bussi, G., Donadio, D., and Parrinello, M. (2007). Canonical sampling through velocity rescaling. J. Chem. Phys. *126*, 014101. https://doi.org/10.1063/1.2408420.

17. Parrinello, M., and Rahman, A. (1981). Polymorphic transitions in single crystals: A new molecular dynamics method. J. Appl. Phys. *52*, 7182–7190. https://doi.org/10.1063/1.328693.

18. Nosé, S., and Klein, M.L. (1983). Constant pressure molecular dynamics for molecular systems. Mol. Phys. *50*, 1055–1076. https://doi.org/10.1080/00268978300102851.

19. Darden, T., York, D., and Pedersen, L. (1993). Particle mesh Ewald: An N ·log(N) method for Ewald sums in large systems. J. Chem. Phys. *98*, 10089–10092. https://doi.org/10.1063/1.464397.

20. Tribello, G.A., Bonomi, M., Branduardi, D., Camilloni, C., and Bussi, G. (2014). PLUMED 2: New feathers for an old bird. Comput. Phys. Commun. *185*, 604–613. https://doi.org/10.1016/j.cpc.2013.09.018.

21. Bonomi, M., Branduardi, D., Bussi, G., Camilloni, C., Provasi, D., Raiteri, P., Donadio, D., Marinelli, F., Pietrucci, F., Broglia, R.A., et al. (2009). PLUMED: a portable plugin for free-energy calculations with molecular dynamics. arXiv. https://doi.org/10.48550/arxiv.0902.0874.

22. Bonomi, M., Bussi, G., Camilloni, C., Tribello, G.A., Banáš, P., Barducci, A., Bernetti, M., Bolhuis, P.G., Bottaro, S., Branduardi, D., et al. (2019). Promoting transparency and reproducibility in enhanced molecular simulations. Nat. Methods *16*, 670–673. https://doi.org/10.1038/s41592-019-0506-8.

23. Humphrey, W., Dalke, A., and Schulten, K. (1996). VMD: visual molecular dynamics. J. Mol. Graph. *14*, 33–38, 27–28. https://doi.org/10.1016/0263-7855(96)00018-5.

24. Wen, J., Pasman, R., Manders, E.M.M., Setlow, P., and Brul, S. (2019). Visualization of Germinosomes and the Inner Membrane in Bacillus subtilis Spores. J. Vis. Exp. : JoVE. https://doi.org/10.3791/59388.

25. Cabrera-Martinez, R.-M., Tovar-Rojo, F., Vepachedu, V.R., and Setlow, P. (2003). Effects of overexpression of nutrient receptors on germination of spores of Bacillus subtilis. J. Bacteriol. *185*, 2457–2464. https://doi.org/10.1128/jb.185.8.2457-2464.2003.

26. Omardien, S., Beek, A.T., Vischer, N., Montijn, R., Schuren, F., and Brul, S. (2018). Evaluating novel synthetic compounds active against Bacillus subtilis and Bacillus cereus spores using Live imaging with SporeTrackerX. Sci. Rep. *8*, 9128. https://doi.org/10.1038/s41598-018-27529-4.

27. Ramirez-Peralta, A., Zhang, P., Li, Y., and Setlow, P. (2012). Effects of Sporulation Conditions on the Germination and Germination Protein Levels of Bacillus subtilis Spores. Appl. Environ. Microbiol. *78*, 2689–2697. https://doi.org/10.1128/aem.07908-11.

28. Maginn, E.J. (2007). Atomistic Simulation of the Thermodynamic and Transport Properties of Ionic Liquids. Acc. Chem. Res. *40*, 1200–1207. https://doi.org/10.1021/ar700163c.

29. Jarzynski, C. (1997). Equilibrium free energy differences from nonequilibrium measurements: a master equation approach. arXiv. https://doi.org/10.48550/arxiv.cond-mat/9707325.

410 30. Cooper, G.R., and Moir, A. (2011). Amino Acid Residues in the GerAB Protein
411 Important in the Function and Assembly of the Alanine Spore Germination Receptor of
412 Bacillus subtilis 168. J. Bacteriol. *193*, 2261–2267. https://doi.org/10.1128/jb.01397-10.

413 31. Yi, X., Liu, J., Faeder, J.R., and Setlow, P. (2011). Synergism between Different
414 Germinant Receptors in the Germination of Bacillus subtilis Spores. J. Bacteriol. *193*, 4664–
415 4671. https://doi.org/10.1128/jb.05343-11.

416 32. Griffiths, K.K., Zhang, J., Cowan, A.E., Yu, J., and Setlow, P. (2011). Germination
417 proteins in the inner membrane of dormant Bacillus subtilis spores colocalize in a discrete
418 cluster. Mol. Microbiol. *81*, 1061–1077. https://doi.org/10.1111/j.1365-2958.2011.07753.x.

419 33. Paidhungat, M., Setlow, B., Driks, A., and Setlow, P. (2000). Characterization of Spores
420 of Bacillus subtilis Which Lack Dipicolinic Acid. J. Bacteriol. *182*, 5505–5512.
421 https://doi.org/10.1128/jb.182.19.5505-5512.2000.

422